An Out-of-Sample Test of the Proposed Link Between Solar Polar Magnetic Fields and M8+ Earthquakes

Oct 6, 2026 · @Bryan Martin

Abstract

Background. Davidson, U-Yen and Holloman (2015) reported that 26 of 33 M8+ earthquakes between 1976 and 2014 fell inside "Significant Windows" derived from Wilcox Solar Observatory (WSO) solar polar field data. The windows covered 41.6% of days, giving $p = 1.5 \times 10^{-5}$. The authors noted that this p-value was biased, because the windows were developed on the same data, and that the model must be judged on future earthquakes.

Methods. We rebuilt the window algorithm from the paper's Appendix A and checked it against the paper's own 1976–2014 statistics. We then froze every rule interpretation and applied the rules to WSO data through January 2026. We scored the nine M8+ earthquakes in the USGS catalogue since January 2014.

Results. In sample, the rebuild flagged 43.2% of days and placed 21 of 30 currently catalogued M8+ events inside windows ($p = 0.003$). Out of sample, the frozen rules flagged 27.8% of days, so chance predicts 2.5 hits; 4 of 9 earthquakes fell inside windows (binomial $p = 0.22$; clustering-preserving $p = 0.21$). The two largest events, the M8.8 Kamchatka (2025) and M8.3 Illapel (2015) earthquakes, fell outside windows.

Conclusion. If the claimed 78.8% hit rate were real, 4 or fewer hits would occur with probability 0.025, and the data favor chance over the claimed rate by about 7 to 1. Across six readings of the ambiguous rules, including the primary one, hits ranged from 2 to 4. The reported association does not persist out of sample and is best explained by windows fitted to the data used to test them.

Keywords: solar polar magnetic field; Wilcox Solar Observatory; great earthquakes; earthquake triggering; out-of-sample validation; overfitting

1. Introduction

Proposals that solar activity triggers large earthquakes recur in the literature, but large statistical studies have found no significant link (Love and Thomas, 2013). The question matters because a real trigger would give a basis for forecasting the most destructive earthquakes.

Davidson, U-Yen and Holloman (2015; hereafter D15) proposed a specific version of the idea. They argued that M8+ earthquakes cluster in "Significant Windows" around extremes and polarity reversals of the Sun's polar magnetic fields, as measured by the Wilcox Solar Observatory (WSO). Between June 1976 and January 2014, 26 of 33 M8+ earthquakes fell inside windows covering 41.6% of days, a result they reported as $p = 1.5 \times 10^{-5}$.

D15 acknowledged that this p-value was biased, because the window rules were refined on the same polar-field record used to test them. They concluded that the model "must [be] assessed by examining how well it predicts large earthquakes in the future" (D15, p. 314). They also proposed widening the rules to capture several near-misses, which would raise the in-sample fit further.

Twelve years of new data now allow the test D15 called for. Nine M8+ earthquakes have occurred since January 2014, and WSO polar-field measurements continue to January 2026. Here we reconstruct the D15 algorithm, verify the reconstruction against D15's own in-sample statistics, freeze it, and score the nine new earthquakes.

2. Data

We use the same two sources as D15, extended to the end of the WSO polar-field record.

Period	Dates	Days	WSO 10-day values	M8+ earthquakes
In sample (D15's period)	Jun 4, 1976 – Jan 17, 2014	13,711 (scored from Jul 5, 1976)	1,375	30 (D15: 33)
Out of sample	Jan 18, 2014 – Jan 9, 2026	4,375	438	9

2.1 Solar polar fields

WSO measures the line-of-sight field in its polemost 3′ apertures, which sample latitudes poleward of about 55°. Every 10 days, the usable daily values in a centered 30-day window are averaged. Like D15, we use the unfiltered north (N) and south (S) values in μT, not the low-pass-filtered series that removes the annual projection effect.

The table was retrieved from wso.stanford.edu/Polar.html on October 6, 2026 (last updated August 10, 2026). It runs from May 31, 1976, to January 9, 2026, 1,813 values in all; later entries are blank. Eighteen interior values were missing and were filled by linear interpolation; the gap nearest any test earthquake ends June 3, 2025, eight weeks before the Kamchatka event.

D15 indexed its series from June 4, 1976, whereas the current WSO table starts on May 31, 1976. We treat this 4-day offset as a sensitivity test (Section 4.3).

2.2 Earthquakes

We retrieved all M ≥ 7.5 events from January 1, 1976, to October 6, 2026, from the USGS ComCat catalog through its FDSN event service on October 6, 2026: 222 events, of which 40 are M ≥ 8.0. The M7.5+ events are needed for D15′s delay rule (Section 3.1); the M8+ events are the test set.

Today′s catalog lists 30 M8+ events in D15′s period, three fewer than D15 used, because magnitudes have since been revised. For example, the August 16, 1976, Mindanao earthquake is now listed at Ms 7.9. Event dates are UTC.

3. Methods

We rebuilt D15′s algorithm from its Appendix A, because the authors′ R code survives only in a web archive we could not reach. Ambiguous rules were settled by matching D15′s own in-sample statistics, and every choice was frozen before any post-2014 earthquake was scored.

3.1 Reconstruction of the window algorithm

The algorithm works on each pole′s 10-day series in five steps:

1. **Long-term extremes.** A 2,000-day running mean is computed, and its local maxima and minima within ±1,000 days mark each cycle′s strongest polar fields.

2. **Annual mini-cycles.** At every point, a linear trend plus a one-year sinusoid is fitted to the surrounding 200 values; the smoothed series U averages all overlapping fits.
3. **Half-minicycles.** The series is cut between consecutive extremes of U, at the point whose field value is closest to the mean of the two extremes.
4. **Spikes.** In each half-cycle the extreme value is a spike, as is any further local extreme separated from it by a dip of more than 10 μT. Spikes within 10 μT of the half-cycle's extreme are primary, and are peaked, semi-flat (a neighbor within 3 μT) or flat (a neighbor equal); half-cycles are single to quadruple by their number of primary spikes.
5. **Polar phases.** A polar maximum turns into a polar minimum when both poles have crossed zero once. The minimum ends at the last return of either pole to its old polarity before the next long-term extreme, and the following polar recovery lasts 1.5 years.

Thirteen conditions then place windows around the spikes and polarity reversals:

Condition	Window centered on	Phase required	Half-width
C1	Primary, peaked spike in a single or double half-cycle	Polar maximum	20 d
C2–C4	Spikes in very strong fields (above 175 μT)	Polar maximum	25 d
C5, C6	Primary, peaked spike in a triple or quadruple half-cycle	Polar maximum	15 d, 10 d
C7, C8, C9	Semi-flat, flat or secondary spike	Any	10 d, 15 d, 10 d
C10	Pole zero crossing with excursions above 15 μT on both sides	Any	15 d
C11	First zero crossing of a pole during a polar maximum	Polar maximum	15 d
C12	End of a polar minimum	Any	15 d
C13	Zero crossing of the average field (N + S)/2	Maximum, or excursions above 50 μT	15 d

Spike windows (C1–C9) also require that the half-cycle does not cross zero and that its peak differs by at least 40 μT from both neighboring half-cycles. Under D15′s delay rule, a window that starts within 30 days after an M8+ earthquake, or of the fourth M7.5+ event within 100 days, is shifted later by 20 days or its half-width, whichever is less. A window starting 31–100 days after such an event shifts by 10 days.

3.2 Interpretation choices

Appendix A leaves four points open, and we settled each as follows:

- **Spike shape** is judged from the two adjacent 10-day values.
- **C13 spacing.** The printed formula appears to require the next average-field reversal within 9 steps, but the text requires reversals to be well separated. We read it as at least 9 steps (90 days), and tested the printed reading and no spacing rule as alternatives.
- **Record ends.** Running means and local fits use whatever data lie within their windows, so they are truncated near the start and end of the record.
- **Dates.** We use WSO′s current dates, and test D15′s 4-day offset as an alternative.

3.3 Calibration and freezing

We compared the rebuild with five statistics D15 reported for 1976–2014: the share of days covered, coverage within each polar phase, the number of half-minicycles per pole, the hit rate, and how the largest events in D15′s Fig. 4 were classified. The reading closest to D15 (C13 at least 90 days, WSO dates) was then frozen.

3.4 Out-of-sample test

The frozen algorithm was run on the full 1976–2026 record, and windows were scored from January 18, 2014, to January 9, 2026. An earthquake is a hit if its UTC date falls inside the union of all windows. Like D15′s, the smoothing is two-sided and uses data after each date, which favors the hypothesis; these windows could not have been drawn in real time.

3.5 Statistical tests

The primary test compares the number of hits k among n earthquakes with the share of days p covered by windows in the same period:

$$P(X \geq k) = \sum_{i=k}^{n} \binom{n}{i} p^{i} (1-p)^{n-i} \tag{1}$$

We also ran three supporting tests:

- **Phase-stratified.** Each earthquake's chance probability is the window coverage within its own polar phase, with the hit count following a Poisson-binomial distribution.
- **Clustering-preserving.** All earthquakes and delay-rule events are shifted together by every possible offset, wrapping within the period (4,375 shifts). Delays are recomputed each time, and p is the share of shifts with at least the observed hits.
- **Against the claimed rate.** The probability of k or fewer hits if D15's 78.8% rate were real, the likelihood ratio between that rate and chance, and the power to reach $p < 0.05$ under the claimed rate.

4. Results

The rebuild reproduces D15's in-sample result, but the frozen rules fail out of sample: 4 of 9 earthquakes fell inside windows, against 2.5 expected by chance.

4.1 Reproduction of the in-sample result

Table 1. D15's reported statistics for 1976–2014 and the same statistics from our rebuild.

Statistic (1976–2014)	D15	Rebuild
Days inside windows	41.6%	43.2%
Days inside windows, polar maximum	46.5%	48.7%
Days inside windows, polar minimum	27.9%	39.3%
Days inside windows, polar recovery	25.2%	16.6%
Half-minicycles, north / south	79 / 75	76 / 68
M8+ earthquakes inside windows	26 of 33 (78.8%)	21 of 30 (70.0%)
Binomial p	1.5×10^{-5}	0.003
Largest events in D15 Fig. 4 classified as D15 reported	—	5 of 6

The rebuild matches D15's overall coverage to within 1.6 percentage points and yields a comparable in-sample signal: p = 0.003, or 0.010 under the clustering-preserving test. The one Fig. 4 disagreement is the September 12, 2007, M8.4 Sumatra earthquake, which falls 14 days from the nearest window in the rebuild. Both April 11, 2012, events fall just outside a window in both versions, as D15 noted.

Phase-level coverage differs most around the 2012–2014 reversal, which the rebuild, with data ending in January 2014, classifies as recovery rather than minimum. As in D15, no in-sample M8+ earthquake occurred during a polar recovery.

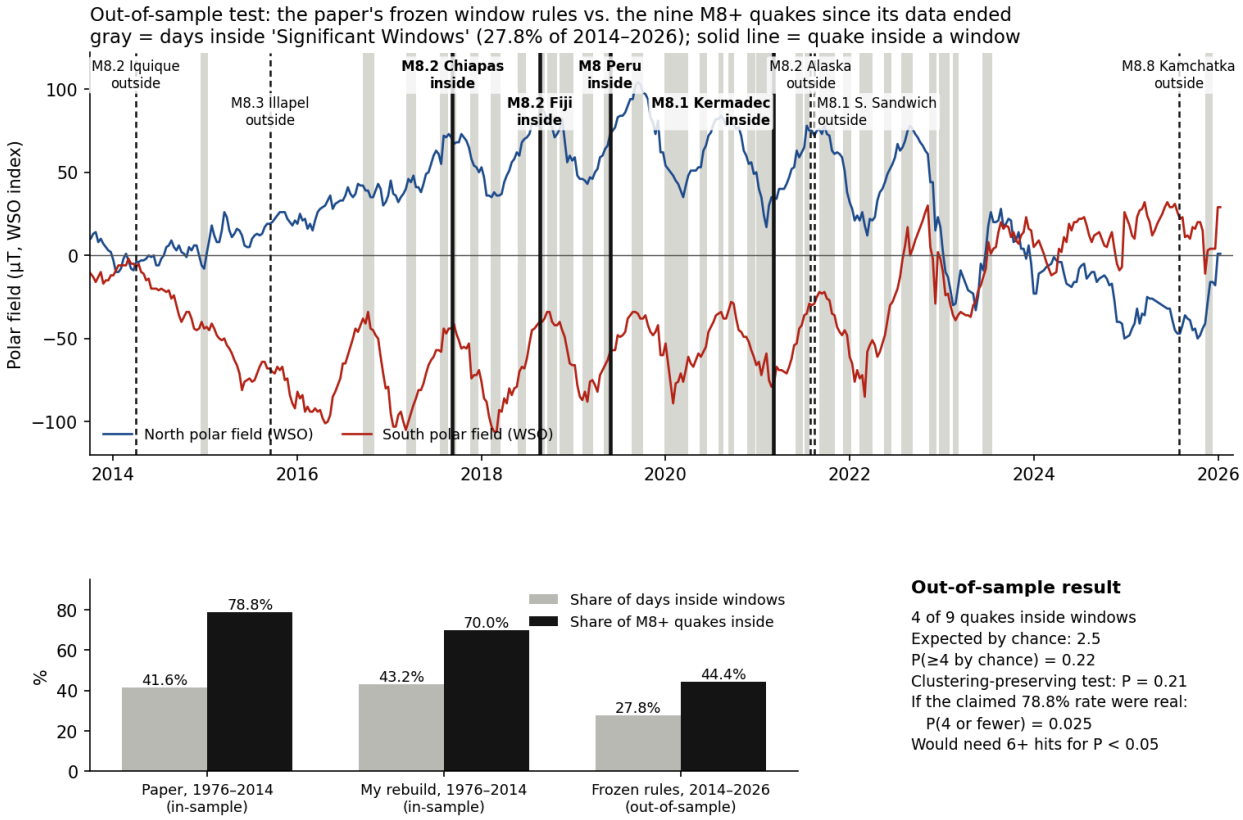
4.2 Out-of-sample performance

The frozen rules covered 27.8% of days between January 18, 2014, and January 9, 2026, so chance predicts 2.5 hits among nine earthquakes. Four fell inside windows (Table 2, Figure 1). The two largest events, Kamchatka (M8.8) and Illapel (M8.3), fell 104 and 247 days from the nearest window.

Table 2. M8+ earthquakes after D15's data ended, newest first. Window conditions are defined in Section 3.1.

Date (UTC)	Earthquake	Magnitude	Polar phase	Result	Distance to nearest window
Jul 29, 2025	Kamchatka Peninsula	8.8	Minimum	Outside	104 d

Date (UTC)	Earthquake	Magnitude	Polar phase	Result	Distance to nearest window
Aug 12, 2021	South Sandwich Islands	8.1	Maximum	Outside	19 d
Jul 29, 2021	Chignik, Alaska	8.2	Maximum	Outside	5 d
Mar 4, 2021	Kermadec Islands	8.1	Maximum	Inside (C7)	0 d
May 26, 2019	Northern Peru	8.0	Maximum	Inside (C13)	0 d
Aug 19, 2018	Fiji (deep)	8.2	Maximum	Inside (C7)	0 d
Sep 8, 2017	Chiapas, Mexico	8.2	Maximum	Inside (C7)	0 d
Sep 16, 2015	Illapel, Chile	8.3	Recovery	Outside	247 d
Apr 1, 2014	Iquique, Chile	8.2	Minimum	Outside	256 d



Data: Wilcox Solar Observatory polar fields (to Jan 2026); USGS catalog. Window rules rebuilt from Davidson, U-Yen & Holloman (2015), Appendix A, and frozen before scoring post-2014 quakes.

Figure 1. Top: WSO north (blue) and south (red) polar fields from 2014 to 2026, with days inside the frozen Significant Windows shaded gray (27.8% of days). Solid vertical lines mark M8+ earthquakes inside a window; dashed lines mark those outside. Bottom: share of days inside windows and share of M8+ earthquakes inside them, for D15's reported in-sample result, our in-sample rebuild, and the out-of-sample test.

Table 3. Statistical tests of the out-of-sample result.

Test	Result
Binomial, against 27.8% coverage (2.5 expected)	P(≥ 4) = 0.22
Phase-stratified (2.9 expected)	P(≥ 4) = 0.32
Clustering-preserving, 4,375 shifts (2.4 expected on average)	P(≥ 4) = 0.21
Polar maximum only: 4 of 6, against 45.1% coverage	P(≥ 4) = 0.26
Probability of 4 or fewer hits if the 78.8% rate were real	0.025
Likelihood ratio, claimed rate against chance	0.14, or about 7 to 1 for chance
Hits needed for p < 0.05	6 of 9
Power to reach p < 0.05 if the 78.8% rate were real	0.90

None of the tests reaches significance. The test was not underpowered: had D15′s rate held, it would have succeeded nine times in ten.

4.3 Robustness

Table 4. Out-of-sample results under alternative readings of the ambiguous rules. The first row is the frozen primary analysis.

C13 spacing rule	Date offset	Days inside windows	Hits of 9	P(≥ hits)
At least 90 days (primary)	0 d	27.8%	4	0.22
At least 90 days	+4 d	27.7%	3	0.47
Within 90 days (as printed)	0 d	22.4%	3	0.33
Within 90 days	+4 d	22.2%	2	0.63
None	0 d	29.1%	4	0.25
None	+4 d	28.9%	3	0.51

No reading gives more than 4 hits or a p-value below 0.2.

Window coverage fell after 2014 for two reasons. Coverage within polar maxima was similar in both periods (48.7% and 45.1%), but 45% of out-of-sample days fell in the long polar minima and recoveries of cycles 24 and 25, where coverage was only 7–8%. Weaker fields also failed the 40 μT amplitude test more often: 55% (north) and 70% (south) of half-cycles passed after 2014, against 86% and 91% before.

5. Discussion

The D15 association behaves like an overfit: strong in the record used to build the rules, absent from new data.

5.1 Why the in-sample signal did not persist

The window rules contain many adjustable parts: 13 conditions, thresholds of 3, 10, 15, 40, 50 and 175 μT, half-widths of 10 to 25 days, and a delay rule. All were developed on the 1976–2014 record. With this much flexibility, a high in-sample hit rate is expected even if no physical link exists.

Temporal clustering makes in-sample fits easier still. Sixteen of the 30 in-sample earthquakes occurred in 2004–2013, so a few well-placed windows capture many events. Accounting for clustering weakens the rebuild's in-sample p-value from 0.003 to 0.010, before any correction for how the rules were chosen.

Out of sample, the hit rate of 44% sits between chance (28%) and the claimed rate (79%), but the likelihood strongly favors chance. Nine events cannot exclude a weak effect, but they reject the effect D15 reported at the 2.5% level.

5.2 Physical plausibility

D15 proposed that the Sun's polar fields charge or discharge the Earth, modeled as a capacitor, and amplify fault stress through piezoelectric effects. But WSO's polar values are an instrument-dependent index of line-of-sight flux near the solar poles, reduced by magnetograph saturation and averaging (Svalgaard et al., 1978; Svalgaard, 2020). The Sun's field reaches Earth only as an interplanetary field of a few nanotesla, thousands of times weaker than Earth's own.

Solid-Earth tides apply far larger and well-characterized stresses, yet they modulate earthquake occurrence only modestly (Ide et al., 2016). Large surveys of solar activity and global seismicity find no significant triggering (Love and Thomas, 2013). Any mechanism that times M8+ ruptures through the polar fields would have to overcome these gaps.

Scope: particles and the global electric circuit. Our test concerns timing, not mechanism. Any effect that follows the polar-field windows would raise the hit rate, whether it acts magnetically, electrically, or through charged particles whose flux the polar fields modulate, such as the solar wind and galactic cosmic rays. Particle effects with their own timing, such as storms driven by coronal mass ejections, high-speed solar-wind streams, and solar energetic particle events, are separate hypotheses that our test does not address.

Evidence on those hypotheses is mixed. Correlations with seismicity have been reported for cosmic-ray detection rates (Homola et al., 2023) and for geomagnetic storms preceding M ≥ 7 earthquakes (Chen et al., 2020). These stand against the null result of Love and Thomas (2013), whose test included solar-wind speed and geomagnetic activity.

D15′s proposed pathway runs through the global electric circuit, in which thunderstorms hold the ionosphere at about 250 kV relative to the ground while a fair-weather current of about 2 pA m^{-2} returns through the atmosphere (Rycroft et al., 2000). Energetic particles modulate this circuit by changing atmospheric conductivity, so it is a genuine route by which solar activity reaches the lower atmosphere. Lithosphere–atmosphere–ionosphere coupling models also invoke the circuit, but to explain proposed precursors that run upward from the crust before earthquakes (Pulinets and Ouzounov, 2011), not stresses imposed from above.

A simple estimate shows the gap that a downward trigger would have to bridge. A current of 2 pA m^{-2} in Earth′s 50 μT field gives a Lorentz force density of about 10^{-16} N m^{-3}, or about 10^{-12} Pa integrated over 10 km of crust; even an assumed storm-time geoelectric field of 10 V km^{-1} in crust with a conductivity of 0.01 S m^{-1} gives less than 10^{-4} Pa. Both are at least seven orders of magnitude below the kilopascal-scale tidal stresses that modulate seismicity only modestly (Ide et al., 2016), and the proposed amplifiers, such as charge concentration at cracks and piezoelectric effects, have not been shown to bridge that gap at fault scale.

5.3 Limitations

- **Reconstruction.** Ours is a reconstruction, not the authors′ code. It differs from D15 in half-cycle counts and phase-level coverage, although it reproduces overall coverage and the in-sample signal.
- **Catalog revisions.** Three of D15′s 33 events are no longer rated M8.0 or above, so the in-sample comparison uses 30 events.
- **Two-sided smoothing.** This favors the hypothesis, and windows near the end of the record, including those around the 2025 Kamchatka earthquake, rest on truncated fits.

- **Power.** At 27.8% coverage, detecting a true hit rate of 60% with 80% power would take about 16 M8+ earthquakes, roughly two decades of data; a rate of 50% would take about 30. Weak effects therefore remain untestable with M8+ events alone.
- **End of the WSO record.** The WSO record ends in January 2026. Future tests need a continuation calibrated to WSO, such as the Kislovodsk STOP series (Berezin and Tlatov, 2026), chosen before any new earthquake is scored.

5.4 Lessons for testing solar–seismic claims

Three practices would have exposed this result in 2015:

- Freeze the rules, data versions, and code before scoring any event, and publish them.
- Test hit rates against the coverage of the windows in the same period, using a null model that preserves earthquake clustering.
- Hold back part of the record, or wait for new events, before claiming significance.

6. Conclusions

1. D15′s window rules, rebuilt from the paper and checked against its own in-sample statistics, place 4 of the 9 M8+ earthquakes since January 2014 inside windows that cover 27.8% of days. Chance predicts 2.5.
2. The result is not significant under any of our tests ($p = 0.21$–0.32). It would be improbable if D15′s 78.8% hit rate were real ($p = 0.025$), and our test had 90% power to confirm that rate.
3. The 2015 association is best explained by flexible windows fitted to the data used to test them. We find no evidence that solar polar magnetic fields time the largest earthquakes.

Data and code availability

WSO polar-field data are available from the Wilcox Solar Observatory. Earthquake data come from the USGS FDSN event service, queried for $M \geq 7.5$ events from January 1, 1976, to October 6, 2026, in CSV format. The analysis code (spf_windows.py and davidson_out_of_sample.py) is available at [repository link to be added].

Acknowledgments

We thank the Wilcox Solar Observatory and J. T. Hoeksema for maintaining the polar-field record, and the USGS for the earthquake catalog. The analysis code and an initial draft were prepared with the assistance of Claude (Anthropic). Funding and prompting by Bryan Martin.

References

- Berezin, I. A., and Tlatov, A. G. (2026). Long-term observations of the solar polar magnetic field with the KMAS/STOP magnetograph: continuing the WSO time series. Research Square preprint. doi:10.21203/rs.3.rs-10957089/v1
- Chen, H., Wang, R., Miao, M., Liu, X., Ma, Y., et al. (2020). A statistical study of the correlation between geomagnetic storms and M ⩾ 7.0 global earthquakes during 1957–2020. *Entropy*, 22(11), 1270. doi:10.3390/e22111270
- Davidson, B., U-Yen, K., and Holloman, C. (2015). Relationship between M8+ earthquake occurrences and the solar polar magnetic fields. *New Concepts in Global Tectonics Journal*, 3(3), 310–322.
- Homola, P., Marchenko, V., Napolitano, A., et al. (2023). Observation of large scale precursor correlations between cosmic rays and earthquakes with a periodicity similar to the solar cycle. *Journal of Atmospheric and Solar-Terrestrial Physics*, 247, 106068. doi:10.1016/j.jastp.2023.106068
- Ide, S., Yabe, S., and Tanaka, Y. (2016). Earthquake potential revealed by tidal influence on earthquake size–frequency statistics. *Nature Geoscience*, 9, 834–837.
- Love, J. J., and Thomas, J. N. (2013). Insignificant solar-terrestrial triggering of earthquakes. *Geophysical Research Letters*, 40, 1165–1170.
- Pulinets, S., and Ouzounov, D. (2011). Lithosphere–Atmosphere–Ionosphere Coupling (LAIC) model: An unified concept for earthquake precursors validation. *Journal of Asian Earth Sciences*, 41(4–5), 371–382.
- Rycroft, M. J., Israelsson, S., and Price, C. (2000). The global atmospheric electric circuit, solar activity and climate change. *Journal of Atmospheric and Solar-Terrestrial Physics*, 62(17–18), 1563–1576.
- Svalgaard, L. (2020). Prediction of Solar Cycle 25. arXiv:2010.02370
- Svalgaard, L., Duvall, T. L., and Scherrer, P. H. (1978). The strength of the Sun's polar fields. *Solar Physics*, 58, 225–239.

- U.S. Geological Survey (2026). ANSS Comprehensive Earthquake Catalog (ComCat). earthquake.usgs.gov, accessed October 6, 2026.
- Wilcox Solar Observatory (2026). WSO polar field observations, 1976–present. wso.stanford.edu/Polar.html, accessed October 6, 2026.